Applied Surface Science 613 (2023) 156030

Contents lists available at ScienceDirect

Applied Surface Science

journal homepage: www.elsevier.com/locate/apsusc

Full length article

Origin of superlubricity promoted by black phosphorus dotted with gold nanoparticles

Gongbin Tang [a,b], Fenghua Su [a,*], Xiaochu Liu [b], Zhongwei Liang [b], Tao Zou [b], Paul K. Chu [c]

[a] School of Mechanical and Automotive Engineering, South China University of Technology, Guangzhou 510640, China
[b] School of Mechanical and Electrical Engineering, Guangzhou University, Guangzhou 510006, China
[c] Department of Physics, Department of Materials Science and Engineering, and Department of Biomedical Engineering, City University of Hong Kong, Tat Chee Avenue, Kowloon, Hong Kong, China

ARTICLE INFO

Keywords:
Black phosphorus
Gold nanoparticles
Superlubricity
Nanofriction

ABSTRACT

Black phosphorus (BP) has attracted considerable attention due to the outstanding mechanical and structural properties. However, the nanoscale frictional properties and atomic-scale mechanism of BP dotted with nanoparticles are still not well understood. Herein, gold nanoparticles (nano-Au) dotted on black phosphorus (Au/BP) are applied as nanoadditives for PAO6 oil to produce macroscale superlubricity at the Si_3N_4/MoN interface. Experiments and molecular dynamics simulation reveal that nano-Au not only enhances adsorption of oil molecules on Au/BP *via* strong hydrogen bonding, but also leads to incommensurate interlayer stacking of BP responsible for the superlubricity. The findings provide fundamental knowledge about the nanoscale frictional behavior as well as superlubricity mechanisms and also reveal a novel concept to design nanoadditives with superlubricity.

1. Introduction

Friction and wear are the main reasons affecting the lifetime of mechanical equipment and energy loss during movement and a state with ultra-low friction and wear is one of the important research topics. Superlubricity representing the most ideal state of friction is defined by a coefficient of friction (COF) of less than 0.01. Superlubricity has been achieved with graphene [1–3], onion-like carbon [4,5], and diamond-like carbon (DLC) [6–8] and recent results reveal that nanocrystalline coatings and nanoadditives with intrinsic catalytic effects can promote degradation of lubricants and transform base oil into carbon-based tribofilms at the friction interface [9–13] to produce outstanding tribological properties.

Black phosphorus (BP) is a burgeoning member of two-dimensional materials with excellent mechanical and tribological properties [14–19]. Our previous study shows that black phosphorus and the corresponding composite nanomaterials catalyze degradation of base oil molecules to form amorphous carbon films when used as lubrication additives [20,21]. Hence, black phosphorus dotted with silver nanoparticles shows synergistic lubrication effects similar to graphene dotted with metal nanoparticles [22,23]. However, the nanoscale friction properties and physical / chemical reactions between BP and nanoparticles at the sliding interface are not well understood. In fact, the role of metal nanoparticles in catalytic production of carbon-based tribofilms is still not clear.

Herein, BP is decorated with gold nanoparticles (nano-Au) by simple chemical reduction to form a lubricating additive (Au/BP). Friction tests demonstrate that PAO oil incorporated with Au/BP produces macroscale superlubricity at the sliding interfaces of Si_3N_4/MoN. Experiments and molecular dynamics (MD) simulation are performed to determine the nano-friction properties of Au/BP and unravel the origin of superlubricity.

2. Results

2.1. Tribological performances

Fig. 1a shows the coefficients of friction (COF) *versus* sliding times for pure PAO6, PAO6 + 0.1 wt% nano-BP (nano-BP-oil), and PAO6+ 0.1 wt % Au/BP (Au/BP-oil). The COF of pure PAO6 oil decreases slowly from 0.08 to 0.03 before stabilizing. The COF of the oil samples containing nano-BP also decrease from 0.1 initially to 0.03. Addition of Au/BP nanoadditives to PAO6 oil produces a COF of about 0.006 after running-in indicative of macroscale superlubricity. Fig. 1b compares the wear

* Corresponding author.
E-mail address: fhsu@scut.edu.cn (F. Su).

https://doi.org/10.1016/j.apsusc.2022.156030
Received 3 November 2022; Received in revised form 30 November 2022; Accepted 6 December 2022
Available online 10 December 2022

rates of the base oil and oil samples with different nanoadditives. The wear rates of the discs lubricated with pure PAO6, PAO6 + 0.1 wt% nano-BP, and PAO6 + 0.1 wt% Au/BP are 1.06×10^{-7} $mm^3(Nm)^{-1}$, 9.28×10^{-8} $mm^3(Nm)^{-1}$, and 5.23×10^{-8} $mm^3(Nm)^{-1}$, respectively. After addition of Au/BP nanoadditives, the tribosystem exhibits superlubricity with the COF and wear rates diminishing significantly. Fig. 1c–h shows the optical images of the wear scar on the bottom disc and test ball lubricated with the three oil samples. As shown in Fig. 1c, the wear track on the friction ball lubricated with PAO6 oil shows many scratches and deep furrows are observed from the corresponding disc (Fig. 1f) indicating that severe abrasive wear occurs during sliding. Fig. 1d, g shows that the wear scars on the friction ball and disc are reduced significantly. In particular, the friction pairs lubricated with Au/BP-oil exhibits the smaller wear scar and better tribological properties (Fig. 1e, h and Fig. 1S).

2.2. Analyses of wear interfaces

To elucidate the mechanism of macroscale superlubricity, SEM, Raman scattering, and XPS are performed to analyze the morphology and chemical composition of the wear track on the test ball as shown in Fig. 2. SEM and EDS (Fig. 2a) show that the wear debris consist of mainly Au, P, and C confirming that Au/BP is deposited on the friction interface. The distribution of C in the wear scar indicates that a carbonaceous film is formed by the tribochemical reaction. The Raman bands D (1334.5 cm^{-1}) and G (1598.8 cm^{-1}) stemming from amorphous carbon are detected from the wear tracks lubricated with nano-BP-oil and Au/BP-oil, as shown in Fig. 2b, suggesting that BP and Au/BP catalyze degradation of PAO6 oil and produce an amorphous carbon film at the sliding interface to reduce friction significantly [20].

XPS is conducted to characterize the chemical states of the solid film on the wear scar lubricated with Au/BP-oil. Fig. 2c shows the survey spectrum revealing the presence of Au, P, C, and O and the protective film is mainly composed of Au/BP nanoadditives and amorphous carbon. The C 1 *s* spectrum (Fig. 2d) shows four peaks at 284.52, 285.40, 286.25, and 288.50 eV corresponding to sp^2 (C-C/C=C), sp^3 (C—C), C—O, and C═O, respectively. Fig. 2e depicts the XPS spectrum of P 2*p*, and the peaks at 130.05 eV and 130.95 eV stem from the $2p_{3/2}$ and $2p_{1/2}$ orbitals of BP. In addition, phosphorus oxide (134.35 and 135.36 eV) is detected and the Au 4*f* (Fig. 2f) spectrum confirms the existence of Au at the friction interfaces. The results reveal that a tribofilm consisting of Au, P, and amorphous carbon is formed at the rubbing surface.

2.3. Nanoscale friction properties and mechanism

To reveal the atomic-scale mechanism of the tribochemical reaction and friction reduction, the adsorption behavior of PAO6 oil molecules on the BP and Au/BP interface is investigated by MD simulation. As shown in Fig. 3a, the adsorbed oil molecules are mainly distributed on the surface of BP and Au/BP. Fig. 3b shows a higher adsorption density for oil molecules near the nano-Au surface indicating the strong attraction of Au-doped BP to oil molecules. The atom-atom radial distribution

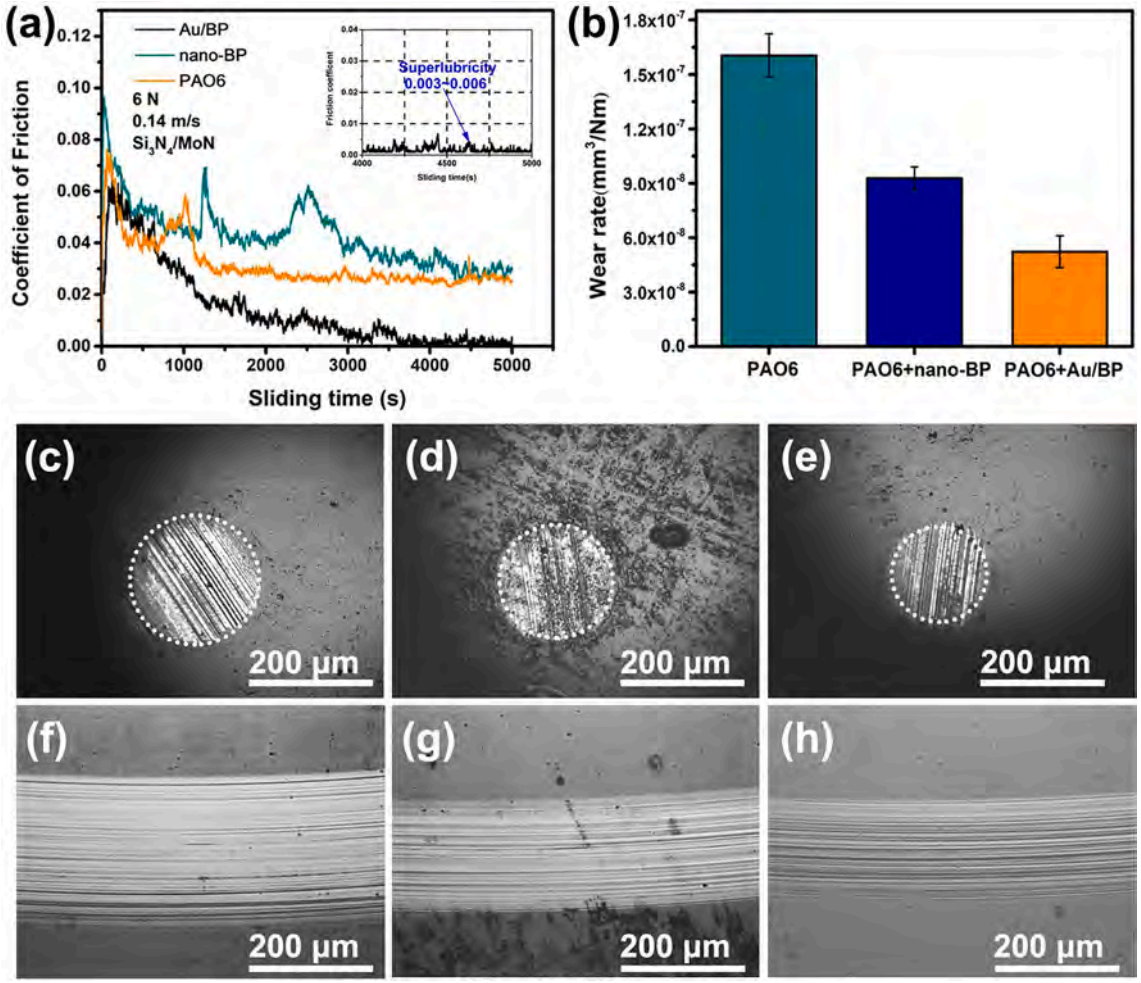

Fig. 1. Tribological properties of the nanoadditives dispersed in PAO oil. (a) Coefficients of friction *versus* sliding times and (b) Wear rates of the pure oil and oil samples with different nanoadditives (Inset showing the partially enlarged view). Optical photos of the wear tracks on (c-e) Bottom discs and (f-h) Corresponding counterpart balls lubricated with different oil samples: (c, f) PAO6 oil, (d, g) nano-BP-oil, and (e, h) Au/BP-oil.

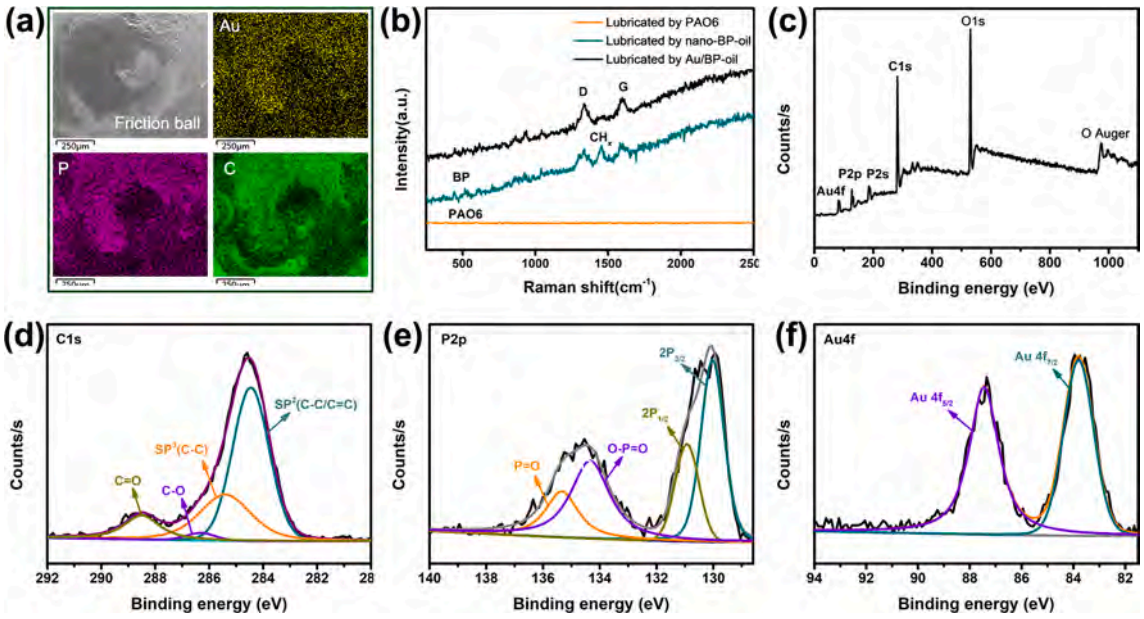

Fig. 2. Characterization of the wear track. (a) SEM and EDS images of the wear scar of the upper ball lubricated with the Au/BP-oil. (b) Raman scattering spectra of the wear scar on the test ball lubricated by different oil samples. (c) XPS survey spectrum of the wear scar on the test ball lubricated with Au/BP, and XPS spectra of (d) C 1 *s*, (e) P 2*p*, and (f) Au 4 *f*.

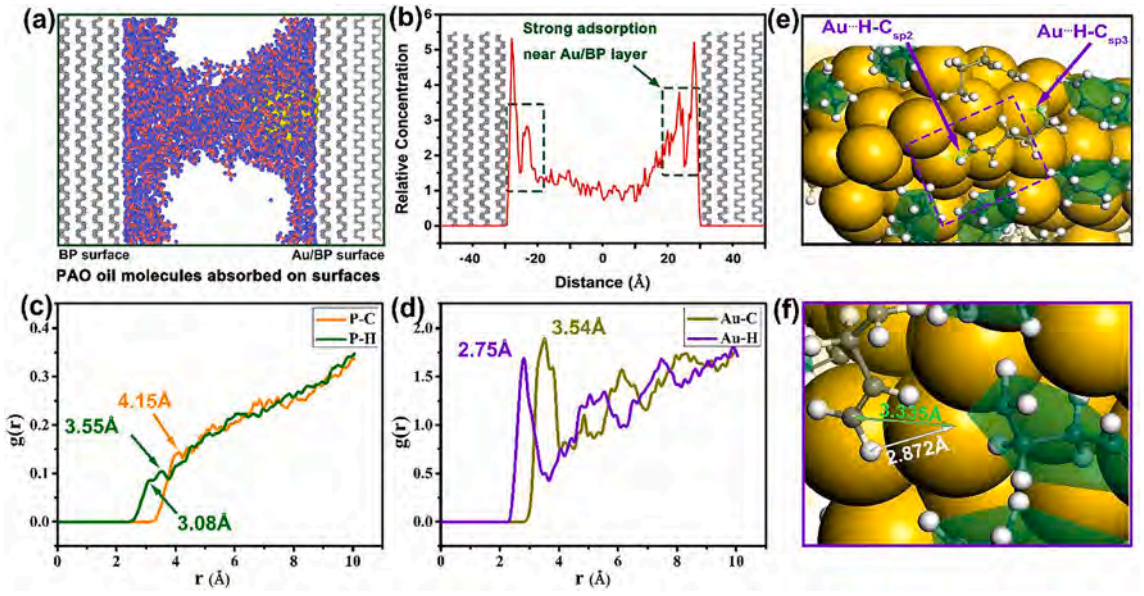

Fig. 3. Adsorption behavior and chemical states. (a) Adsorption snapshots and (b) Relative concentration distributions. (c, d) Radial distribution functions g(r) for atomic distances: P—C, P—H, Au—C, and Au—H. (e, f) Snapshots from MD simulation with the yellow, gray, and white spheres representing gold, carbon, and hydrogen atoms, respectively. (For interpretation of the references to colour in this figure legend, the reader is referred to the web version of this article.)

functions (RDFs) is analyzed to study the interactions between PAO oil and nanoadditives. Fig. 3c shows that the peaks of P—H appear between 3.08 Å and 3.55 Å and most of the C atoms are distributed beyond 4 Å from the P atoms, disclosing that oil molecules absorb onto the BP surface *via* weak electrostatic P···H-C interactions [24]. In contrast, the Au—H RDF peak at 2.75 Å and Au—C RDF peak at 3.54 Å (Fig. 3d) arise from strong Au···H-C hydrogen bonding [25–27]. The details about the interactions between oil molecules and nano-Au are described in Fig. 3e, f. It is evident that H atoms on both ends of the oil molecules adsorb on the Au surface at a distance of 2.68– 2.87 Å, forming stable hydrogen bonds of Au···H-C_{sp2} and Au···H-C_{sp3}. Hence, the Au—H bond plays a crucial role in the strong adsorption of PAO oil molecules at the Au/BP interface and formation of a stable lubricating film. This strong interaction ensures that nano-Au can capture free H atoms *via* dehydrogenation of PAO during the friction process to further promote degradation of oil molecules and formation of amorphous carbon films to reduce friction and wear.

The nanoscale tribological properties of Au/BP-oil are determined to elucidate the superlubricity mechanism. Fig. 4a, b shows the friction force of BP and Au/BP generated by MD simulation for oil molecule lubrication. As shown in Fig. 4a, the friction force of the BP increases with sliding and addition of nano-Au to the BP surface reduces the friction force (Fig. 4b), which is consistent with the tribological test results (Fig. 1a). The potential energy surface (PES) of BP and stress

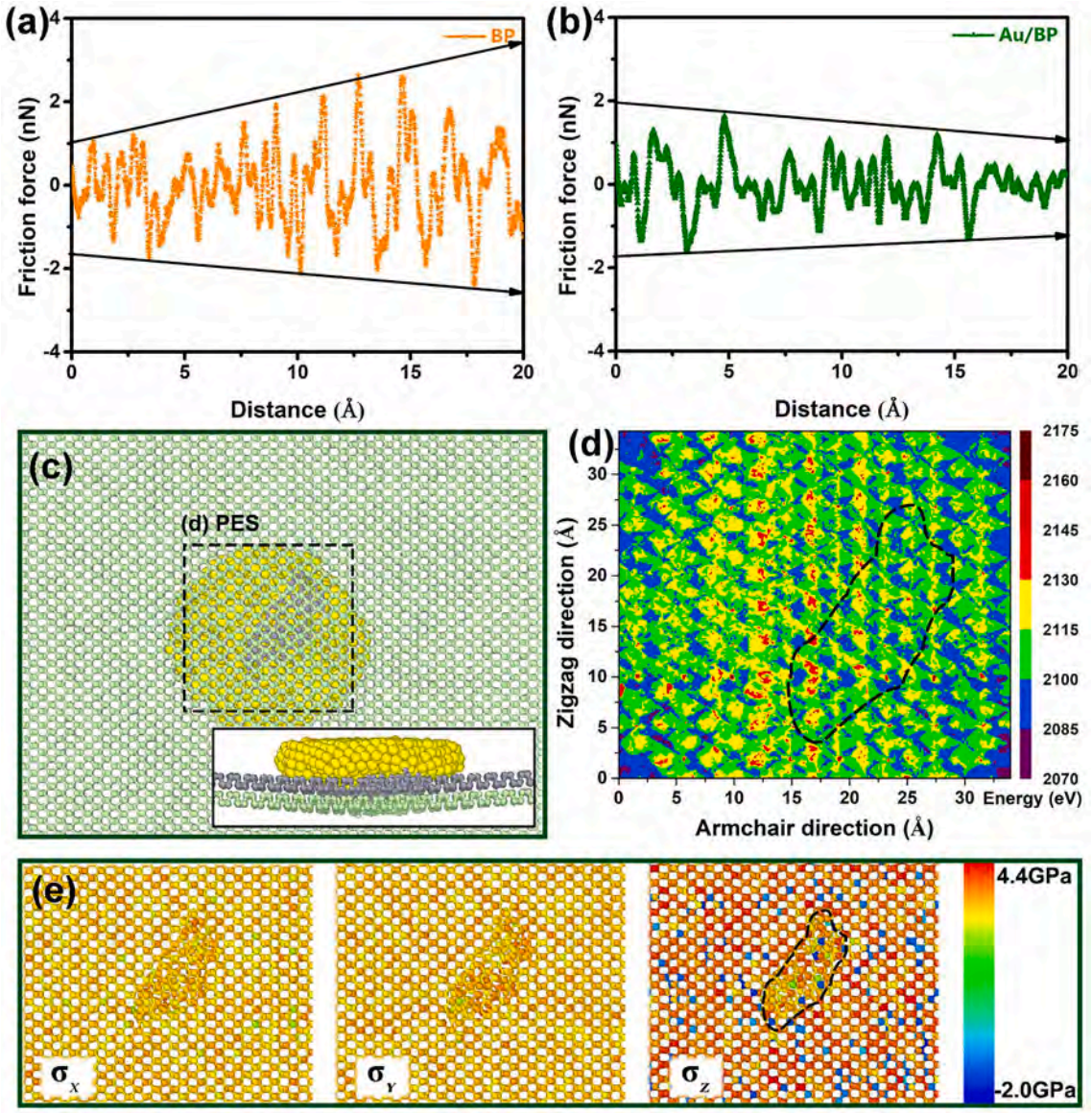

Fig. 4. Nanoscale tribololgical properties. Curve of friction force *versus* sliding distance for (a) Nano-BP-oil and (b) Au/BP-oil. (c) Top view of the snapshot in friction simulation showing the incommensurate atomic contact. (d) PES of the selected area in(c). (e) Stress distributions of σ_x, σ_y, and σ_z.

distribution are calculated to explain friction reduction and Fig. 4c describes the details of the rubbing interfaces in the MD simulation. The oil molecules are hidden in the snapshot to reveal the structural details of the phosphorus and Au atoms. The structure of the P atoms changes in the contact area leading to the transition from commensurate to incommensurate contacts [28]. Fig. 4d shows that in the contact area, the energy decreases because the atoms cannot lock into the local registry at the surface [29,30] consequently reducing the potential barrier of sliding. According to the stress distribution in Fig. 4e, the stress also decreases in the contact region where the structure of the P atoms changes, especially for σ_z. Reduction of the potential barriers, friction force, and stress indicates that nano-Au changes the parallel angle and stacking mode between BP layers contributing to the superlubricity. To summarize, MD simulation reveals that addition of nano-Au to the BP surface enhances absorption of Au/BP and PAO oil, and leads to random incommensurate stacking, producing superlubricity.

3. Discussion

Decorating 2D materials with gold nanoparticles has been shown to produce excellent tribological properties for Au/graphene oxide [22] and Au/MoS_2 [31,32]. However, previous works have mainly focused on the role of gold nanoparticles in repairing the wear scar and improving the load capacity. Herein, we reveal that nano-Au on the BP surface has unique physical and chemical properties as a lubricating nanoadditive and they are the main reasons for the superlubricating state. In the case of lubrication with PAO oil containing pristine BP, the nanosheets are deposited on the interface to fill and repair the wear scar. The deposited BP is oxidized partially and the oil molecules bond to oxide on the BP surface through hydrogen bonding [33] to provide reactive sites for decomposition of oil molecules and formation of the amorphous carbon-based tribofilms (Fig. 2b). After BP is dotted with Au nanoparticles, oil molecules adsorb quickly onto the composite nano-additives by hydrogen bonding to form a robust lubricating film (Fig. 3a, b). It is worth pointing out that the strong interactions of Au and H atoms facilitate recombination of PAO oil molecules to form a carbon-based lubricating film during the friction test. As sliding proceeds, incommensurate stacking induced by nano-Au (Fig. 4c) plays a significant role in minimizing the friction and wear to achieve superlubricity.

In recapitulation, experiments and MD simulation are performed to

investigate the nanoscale friction behavior of Au/BP-oil and the corresponding superlubricity mechanism on the atomic scale. Nano-Au not only enhances the interactions between the nanoadditives and oil molecules, but also improves degradation of oil molecules and formation of carbon-based lubricating films to reduce wear. In addition, an amorphous and incommensurate atomic contact is formed by nano-Au under high stress and shear, ultimately driving the tribosystem to superlubricity. The results provide fundamental knowledge about the origin of superlubricity promoted by BP dotted with nano-Au and reveal a novel method for designing nanoaddtivies with superlubricity.

4. Materials and methods

4.1. Synthesis of materials

The BP nanosheets were prepared by a liquid phase exfoliation process described previously [20]. In the typical experiments, 50 mg of $AuHCl_4{\cdot}4H_2O$ and 100 mg of BP nanosheets were added to the NMP solution and magnetically stirred at 80 rpm for 0.5 h. The Au/BP nanocomposite was collected by centrifugation and washed with absolute ethanol. For comparison, nano-BP was synthesized by the same method but without $AuHCl_4{\cdot}4H_2O$. Fig. 2S and Fig. 3S reveal successful preparation of nano-BP and Au/BP and Fig. 3S shows that the size of the BP nanosheet and nano-Au is approximately 200 nm and 20 nm, respectively. The friction ball with a diameter of 6.0 mm was made of Si_3N_4 (Ra about 20 nm). The disc with a sliding contact radius of 5 mm was composed of MoN (Ra is approximately 20 nm) fabricated by ourselves [34].

4.2. Tribological assessment

The tribological test was carried out on a ball-on-plate tribometer (UMT-TriboLab, Bruker, USA) and the nanomaterials were modified with oleic acid to improve the dispersibility in PAO oil. 1 mg of Au/BP was mixed with 0.1 ml of oleic acid and stirred for 0.5 h at 60 °C. The mixture was washed with a large amount of ethanol to remove excess oleic acid and then dried for 8 h in vacuum at 60 °*C. prior* to the test, the base oil of PAO6 was mixed with Au/BP and sonicated for 30 min to prepare the nanofluid lubricant. The friction and wear tests were performed under a loading of 6.0 N at a rotation speed of 200 rpm at least 5 times to obtain averages (25 °C, 20–25% RH). The wear rate (W_r) of the disc was calculated by the following formula: $W_r = V/(S \cdot F)$, in which W_r, V, S and F are the wear rate, wear volume, sliding distance, and normal load, respectively.

4.3. Characterization

The structure of the nanomaterials was characterized by X-ray diffraction (XRD) on a Philips X'pert X-ray diffractometer (Cu K_α radiation) at 40 kV and 40 mA from 5^o to 90^o. The Raman scattering spectra were acquired on the Dilor Labram-1B multichannel confocal microspectrometer equipped with the 532 nm and 20 mW laser. The morphology and microstructure were examined by transmission electron microscopy (TEM, FEI Technai F20) and scanning electron microscope (SEM, Nova NanoSEM430). The micromorphology of the wear tracks on the friction pairs was characterized by optical microscopy (CCM-600E), 3D profilometry (RTEC UP Dual-Mode, America), and scanning electron microscopy (SEM, Nova NanoSEM430), and the phase composition and elemental composition were determined by XRD and XPS, respectively.

4.4. Molecular dynamics simulation

Molecular Dynamics simulation was employed to investigate the adsorption properties and atomic-scale tribological behavior of the lubricating materials at the friction interface. The adsorption characteristics of the friction system were simulated by the Forcite module in the Materials Studio software. The size of the model was 39.7 Å × 63.4 Å × 101.2 Å. The PAO6 oil molecules and gold nanoparticles with a diameter of 20 nm were sandwiched between the BP layers to simulate adsorption. The PAO6 oil molecules were simplified and replaced by *n*-Pentane (C_5H_{10}) [35]. The model adopted periodic boundaries in *x* and *y* directions and Nose´−Hoover canonical (NVT) thermostatic simulator with a time step of 1.0 fs. The simulation process consisted of three steps. (1) Firstly, the friction system was relaxed for 100 ps at 298 K to reach equilibrium. In this simulation step, the outer layer of BP was treated as a rigid body. (2) The temperature of the system was raised slowly to 500 K to simulate the local high temperature at the friction interface and this step proceeded for 100 ps. (3) The system was simulated for 1.0 ns at 500 K. In the simulation, the interaction between atoms was Lennard Jones and the cutoff was set to 12.5 Å. In the model, the numbers of P and Au atoms were 5760 and 272 respectively, and the number of oil molecules was 500 for a total of 13,532 atoms.

The nanoscale tribological properties of the nanoadditives and oil were studied by the LAMMPS software package. The friction force, stress distribution, and the potential surface energy of BP are calculated. Fig. S4 shows the molecular dynamics model for simulating and calculating the sliding process with a size of 126.9 Å × 99.4 Å × 149.5 Å. The upper BP in the model was divided into a moving layer, constant temperature layer (NVT), and Newton layer (NVE) and the lower black phosphorus was divided into the fixed layer, constant-temperature layer, and Newton layer. The oil molecules in the middle, nano-Au, and BP on the contact surface were set as Newton layers. The time step in the was 1 fs. In the simulation, the interactions between different atoms were Lennard-Jones and the cutoff was 12.5 Å. The potential well depth (ε) and the van der Waals separation distance (σ) parameters of the Lennard-Jones potentials interactions for P-C, P-H, and P-P (BP layers interactions) are (0.006878 eV, 3.4225 Å), (0.005023 eV, 3.3128 Å), and (0.01594 eV, 3.3438 Å), respectively [36,37]. The Stillinger-Weber potentials [38] were adopted between the single layers of BP and the Lennard-Jones potentials were used between layers. The AIREBO potentials was used between oil molecules [39] and the EAM potentials were used between Au nanoparticles [40]. The simulation process included three steps: (1) The friction system was relaxed at 300 K for 100 ps and in this step, the outer layer of BP was treated as a rigid body. (2) A normal load was applied to the top boundary to compress the system to a pressure of 1.0 GPa in the *z*-direction. (3) The top BP layer was subjected to a constant sliding speed of 10 m/s, while the lower BP was a rigid body. This step proceeded for 1 ns. The loads applied in the second stage and third stage were the same. In the model, the numbers of P and Au atoms were 57,600 and 272, respectively, and the number of oil molecules was 500 for a total of 63,572 atoms. Similar to the previous steps, a similar model was established to simulate the tribological properties of BP and oil molecules in the friction process as the control group. The open source software OVITO was used in data and visual processing [41].

CRediT authorship contribution statement

Gongbin Tang: Methodology, Conceptualization, Visualization, Writing – original draft. **Fenghua Su:** Conceptualization, Resources. **Xiaochu Liu:** Investigation, Data curation. **Zhongwei Liang:** Methodology, Visualization. **Tao Zou:** Methodology, Supervision. **Paul K. Chu:** Resources, Supervision, Writing – review & editing.

Declaration of Competing Interest

The authors declare that they have no known competing financial interests or personal relationships that could have appeared to influence the work reported in this paper.

Data availability

The data that has been used is confidential.

Acknowledgments

The authors acknowledge financial support from the National Natural Science Foundation of China (52175168), Natural Science Foundation of Guangdong Province (2021A1515012266), City University of Hong Kong Donation Research Grant (DON-RMG No. 9229021) and City University of Hong Kong Strategic Research Grant (SRG No. 7005505).

Appendix A. Supplementary data

Supplementary data to this article can be found online at https://doi.org/10.1016/j.apsusc.2022.156030.

References

[1] D. Berman, S.A. Deshmukh, S.K. Sankaranarayanan, A. Erdemir, A.V. Sumant, Macroscale superlubricity enabled by graphene nanoscroll formation, Science 348 (2015), https://doi.org/10.1126/science.1262024.
[2] Y. Liu, J. Li, X. Ge, S. Yi, H. Wang, Y. Liu, J. Luo, Macroscale superlubricity achieved on the hydrophobic graphene coating with glycerol, ACS Appl. Mater. Interfaces 12 (2020) 18859–18869, https://doi.org/10.1021/acsami.0c01515.
[3] S.-W. Liu, H.-P. Wang, Q. Xu, T.-B. Ma, G. Yu, C. Zhang, D. Geng, Z. Yu, S. Zhang, W. Wang, Y.-Z. Hu, H. Wang, J. Luo, Robust microscale superlubricity under high contact pressure enabled by graphene-coated microsphere, Nat. Commun. 8 (2017) 14029, https://doi.org/10.1038/ncomms14029.
[4] D. Berman, B. Narayanan, M.J. Cherukara, S.K.R.S. Sankaranarayanan, A. Erdemir, A. Zinovev, A.V. Sumant, Operando tribochemical formation of onion-like-carbon leads to macroscale superlubricity, Nat. Commun. 9 (2018) 1164, https://doi.org/10.1038/s41467-018-03549-6.
[5] Z. Gong, C. Bai, L. Qiang, K. Gao, J. Zhang, B. Zhang, Onion-like carbon films endow macro-scale superlubricity, Diam. Relat. Mater. 87 (2018) 172–176, https://doi.org/10.1016/j.diamond.2018.06.004.
[6] S. Yi, X. Chen, J. Li, Y. Liu, S. Ding, J. Luo, Macroscale superlubricity of Si-doped diamond-like carbon film enabled by graphene oxide as additives, Carbon 176 (2021) 358–366, https://doi.org/10.1016/j.carbon.2021.01.147.
[7] K. Wang, J. Zhang, T. Ma, Y. Liu, A. Song, X. Chen, Y. Hu, R.W. Carpick, J. Luo, Unraveling the friction evolution mechanism of diamond-like carbon film during nanoscale running-in process toward superlubricity, Small 17 (2021) 2005607, https://doi.org/10.1038/srep46394.
[8] M.I. De Barros Bouchet, J.M. Martin, J. Avila, M. Kano, K. Yoshida, T. Tsuruda, S. Bai, Y. Higuchi, N. Ozawa, M. Kubo, M.C. Asensio, Diamond-like carbon coating under oleic acid lubrication: evidence for graphene oxide formation in superlow friction, Sci. Rep. 7 (2017) 46394, https://doi.org/10.1038/srep46394.
[9] A. Erdemir, G. Ramirez, O.L. Eryilmaz, B. Narayanan, Y. Liao, G. Kamath, S. K. Sankaranarayanan, Carbon-based tribofilms from lubricating oils, Nature 536 (2016) 67–71, https://doi.org/10.1038/nature18948.
[10] X. Xu, Z. Xu, J. Sun, G. Tang, F. Su, In situ synthesizing carbon-based film by tribo-induced catalytic degradation of poly-α-olefin oil for reducing friction and wear, Langmuir 36 (2020) 10555–10564, https://doi.org/10.1021/acs.langmuir.0c01896.
[11] N. Argibay, T. Babuska, J. Curry, M. Dugger, P. Lu, D. Adams, B. Nation, B. Doyle, M. Pham, A. Pimentel, In-situ tribochemical formation of self-lubricating diamond-like carbon films, Carbon 138 (2018) 61–68, https://doi.org/10.1016/j.carbon.2018.06.006.
[12] Q. Chang, P. Rudenko, D.J. Miller, J. Wen, D. Berman, Y. Zhang, B. Arey, Z. Zhu, A. Erdemir, Operando formation of an ultra-low friction boundary film from synthetic magnesium silicon hydroxide additive, Tribol. Int. 110 (2017) 35–40, https://doi.org/10.1016/j.triboint.2017.02.003.
[13] C. Liu, X. Gu, L. Yang, X. Song, M. Wen, J. Wang, Q. Li, K. Zhang, W. Zheng, C. Chen, Ultralow-friction and ultralow-wear TiN-Ag solid solution coating in base oil, J. Phys. Chem. Lett. 11 (2020) 1614–1621, https://doi.org/10.1021/acs.jpclett.9b03864.
[14] W. Wang, G. Xie, J. Luo, Superlubricity of black phosphorus as lubricant additive, ACS Appl. Mater. Interfaces 10 (2018) 43203–43210, https://doi.org/10.1021/acsami.8b14730.
[15] J. Li, S. Yi, K. Wang, Y. Liu, J. Li, Alkene-catalyzed rapid layer-by-layer thinning of black phosphorus for precise nanomanufacturing, ACS Nano 16 (2022) 13111–13122, https://doi.org/10.1021/acsnano.2c05909.
[16] S. Wu, F. He, G. Xie, Z. Bian, J. Luo, S. Wen, Black phosphorus: degradation favors lubrication, Nano Lett. 18 (2018) 5618–5627, https://doi.org/10.1021/acs.nanolett.8b02092.
[17] S. Yi, J. Li, J. Rao, X. Ma, Y. Zhang, Alkyl-functionalized black phosphorus nanosheets triggers macroscale superlubricity on diamond-like carbon film, Chem. Eng. J. 449 (2022), 137764, https://doi.org/10.1016/j.cej.2022.137764.
[18] Q. Li, F. Su, G. Tang, X. Xu, Y. Chen, J. Sun, Atomic-scale friction of black phosphorus from first-principles calculations: insensitivity of friction under the high-load, Tribol. Int. 172 (2022), 107590, https://doi.org/10.1016/j.triboint.2022.107590.
[19] J. Li, J. Li, Synergistic lubrication effect between oxidized black phosphorus and oil molecules triggers superlubricity, J. Phys. Chem. Lett. 13 (2022) 8245–8253, https://doi.org/10.1021/acs.jpclett.2c02144.
[20] G. Tang, F. Su, X. Xu, P.K. Chu, 2D black phosphorus dotted with silver nanoparticles: an excellent lubricant additive for tribological applications, Chem. Eng. J. 392 (2020), 123631, https://doi.org/10.1016/j.cej.2019.123631.
[21] G. Tang, Z. Wu, F. Su, H. Wang, X. Xu, Q. Li, G. Ma, P.K. Chu, Macroscale superlubricity on engineering steel in the presence of black phosphorus, Nano Lett. 21 (2021) 5308–5315, https://doi.org/10.1021/acs.nanolett.1c01437.
[22] Y. Meng, F. Su, Y. Chen, Au/graphene oxide nanocomposite synthesized in supercritical CO2 fluid as energy efficient lubricant additive, ACS Appl. Mater. Interfaces 9 (2017) 39549–39559, https://doi.org/10.1021/acsami.7b10276.
[23] Y. Meng, F. Su, Y. Chen, Synthesis of nano-Cu/graphene oxide composites by supercritical CO2-assisted deposition as a novel material for reducing friction and wear, Chem. Eng. J. 281 (2015) 11–19, https://doi.org/10.1016/j.cej.2015.06.073.
[24] Y. Lu, Y. Hong, Z. Xu, H. Liu, Interfacial interactions and structures of imidazolium-based ionic liquids on black phosphorus surface from first-principles, J. Mol. Liq. 335 (2021), 116562, https://doi.org/10.1016/j.molliq.2021.116562.
[25] H. Darmandeh, J. Löffler, N.V. Tzouras, B. Dereli, T. Scherpf, K.S. Feichtner, S. Vanden Broeck, K. Van Hecke, M. Saab, C.S. Cazin, Au··· H− C hydrogen bonds as design principle in gold (I) catalysis, Angew. Chem. 133 (2021) 21182–21192, https://doi.org/10.1002/ange.202108581.
[26] M. Kumar, J.S. Francisco, Evidence of the elusive gold-induced non-classical hydrogen bonding in aqueous environments, J. Am. Chem. Soc. 142 (2020) 6001–6006, https://doi.org/10.1021/jacs.9b05493.
[27] M.F. Camellone, D. Marx, Solvation of Au+ versus Au 0 in aqueous solution: electronic structure governs solvation shell patterns, Phys. Chem. Chem. Phys. 14 (2012) 937–944, https://doi.org/10.1039/C1CP22961C.
[28] G. Losi, P. Restuccia, M.C. Righi, Superlubricity in phosphorene identified by means of ab initio calculations, 2D Mater. 7 (2020), 025033, https://doi.org/10.1088/2053-1583/ab72d7.
[29] B. Luan, M.O. Robbins, The breakdown of continuum models for mechanical contacts, Nature 435 (2005) 929–932, https://doi.org/10.1038/nature03700.
[30] M.H. Müser, L. Wenning, M.O. Robbins, Simple microscopic theory of Amontons's laws for static friction, Phys. Rev. Lett. 86 (2001) 1295–1298, https://doi.org/10.1103/PhysRevLett.86.1295.
[31] P. Stoyanov, S. Gupta, R.R. Chromik, J.R. Lince, Microtribological performance of Au–MoS2 nanocomposite and Au/MoS2 bilayer coatings, Tribol. Int. 52 (2012) 144–152, https://doi.org/10.1016/j.triboint.2012.03.014.
[32] T.W. Scharf, R.S. Goeke, P.G. Kotula, S.V. Prasad, Synthesis of Au–MoS2 nanocomposites: thermal and friction-induced changes to the structure, ACS Appl. Mater. Interfaces 5 (2013) 11762–11767, https://doi.org/10.1021/am4034476.
[33] Y. Gu, T. Kar, S. Scheiner, Fundamental properties of the CH···O interaction: is it a true hydrogen bond? J. Am. Chem. Soc. 121 (1999) 9411–9422, https://doi.org/10.1021/ja991795g.
[34] X. Xu, F. Su, Z. Li, Microstructure and tribological behaviors of MoN-Cu nanocomposite coatings sliding against Si3N4 ball under dry and oil-lubricated conditions, Wear 434 (2019), 202994, https://doi.org/10.1016/j.wear.2019.202994.
[35] X. Li, A. Wang, K.-R. Lee, Role of unsaturated hydrocarbon lubricant on the friction behavior of amorphous carbon films from reactive molecular dynamics study, Comput. Mater. Sci. 161 (2019) 1–9, https://doi.org/10.1016/j.commatsci.2019.01.032.
[36] S.J.V. Frankland, V.M. Harik, G.M. Odegard, D.W. Brenner, T.S. Gates, The stress–strain behavior of polymer–nanotube composites from molecular dynamics simulation, Compos. Sci. Technol. 63 (2003) 1655–1661, https://doi.org/10.1016/S0266-3538(03)00059-9.
[37] Y. Liu, Y. Liu, J. Luo, Atomic scale simulation on the fracture mechanism of black phosphorus monolayer under indentation, Nanomaterials 8 (2018) 682, https://doi.org/10.3390/nano8090682.
[38] J.-W. Jiang, H.S. Park, Negative poisson's ratio in single-layer black phosphorus, Nat. Commun. 5 (2014) 1–7, https://doi.org/10.1038/ncomms5727.
[39] S.J. Stuart, A.B. Tutein, J.A. Harrison, A reactive potential for hydrocarbons with intermolecular interactions, J. Chem. Phys. 112 (2000) 6472–6486, https://doi.org/10.1063/1.481208.
[40] S.M. Foiles, M.I. Baskes, M.S. Daw, Embedded-atom-method functions for the fcc metals Cu, Ag, Au, Ni, Pd, Pt, and their alloys, Phys. Rev. B 33 (1986) 7983–7991, https://doi.org/10.1103/PhysRevB.33.7983.
[41] A. Stukowski, Visualization and analysis of atomistic simulation data with OVITO–the open visualization tool, Model. Simul. Mater. Sci. Eng. 18 (2009), 015012, https://doi.org/10.1088/0965-0393/18/1/015012.

Supplementary Information

Origin of Superlubricity Promoted by Black Phosphorus dotted with Gold Nanoparticles

Gongbin Tang [a, b], Fenghua Su*[, a], Xiaochu Liu [b], Zhongwei Liang [b], Tao Zou [b], Paul K. Chu [c]

[a] School of Mechanical and Automotive Engineering, South China University of Technology, Guangzhou 510640, China

[b] School of Mechanical and Electrical Engineering, Guangzhou University, Guangzhou 510006, China

[c] Department of Physics, Department of Materials Science and Engineering, and Department of Biomedical Engineering, City University of Hong Kong, Tat Chee Avenue, Kowloon, Hong Kong, China

*** Corresponding Author： Prof. Fenghua Su**, Email:fhsu@scut.edu.cn; Tel. /Fax.: +86-20-82313996; ORCiD: 0000-0002-6953-4663

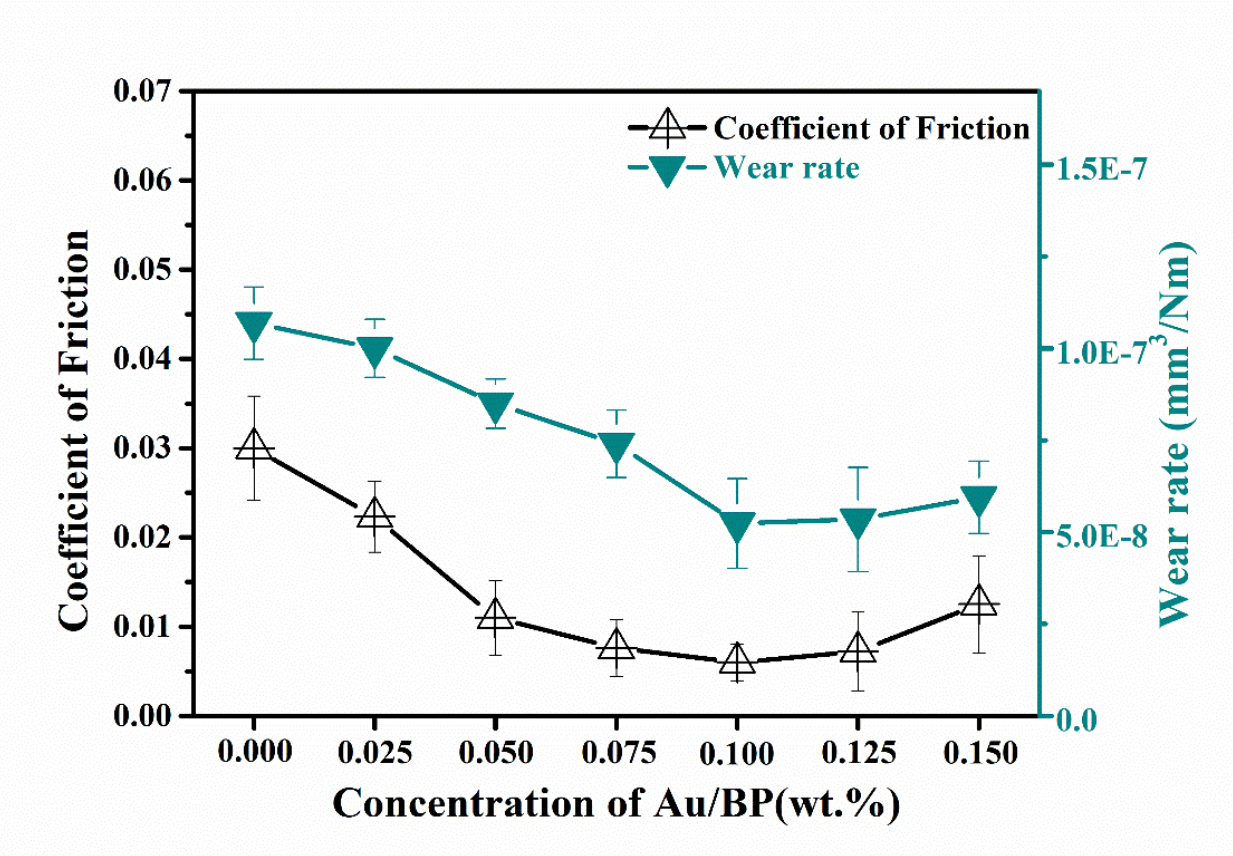

Figure 1S. Stability of superlubricity for different concentrations. Figure 1S shows the average friction coefficients and wear rates of the oil samples for different concentrations of Au/BP. Superlubricity can be achieved when the concentration of Au/BP is between 0.075 and 0.125 wt%. The curves of COFs and wear rates show a 'deep valley' with increasing Au/BP in the base oil. The COFs and wear rates decrease gradually with increasing Au/BP concentrations from 0 to 0.1 wt%, but increasing the amount of Au/BP to 0.15 wt% increases both the COFs and wear rates. This phenomenon is attributed to that nanoadditives are involved in the friction interface with oil molecules and then deposition and aggregation appear in the grooves of the friction pair. Excessive Au/BP accumulation at the friction interface hinders lubrication of oil molecules resulting in larger COFs and wear rates.

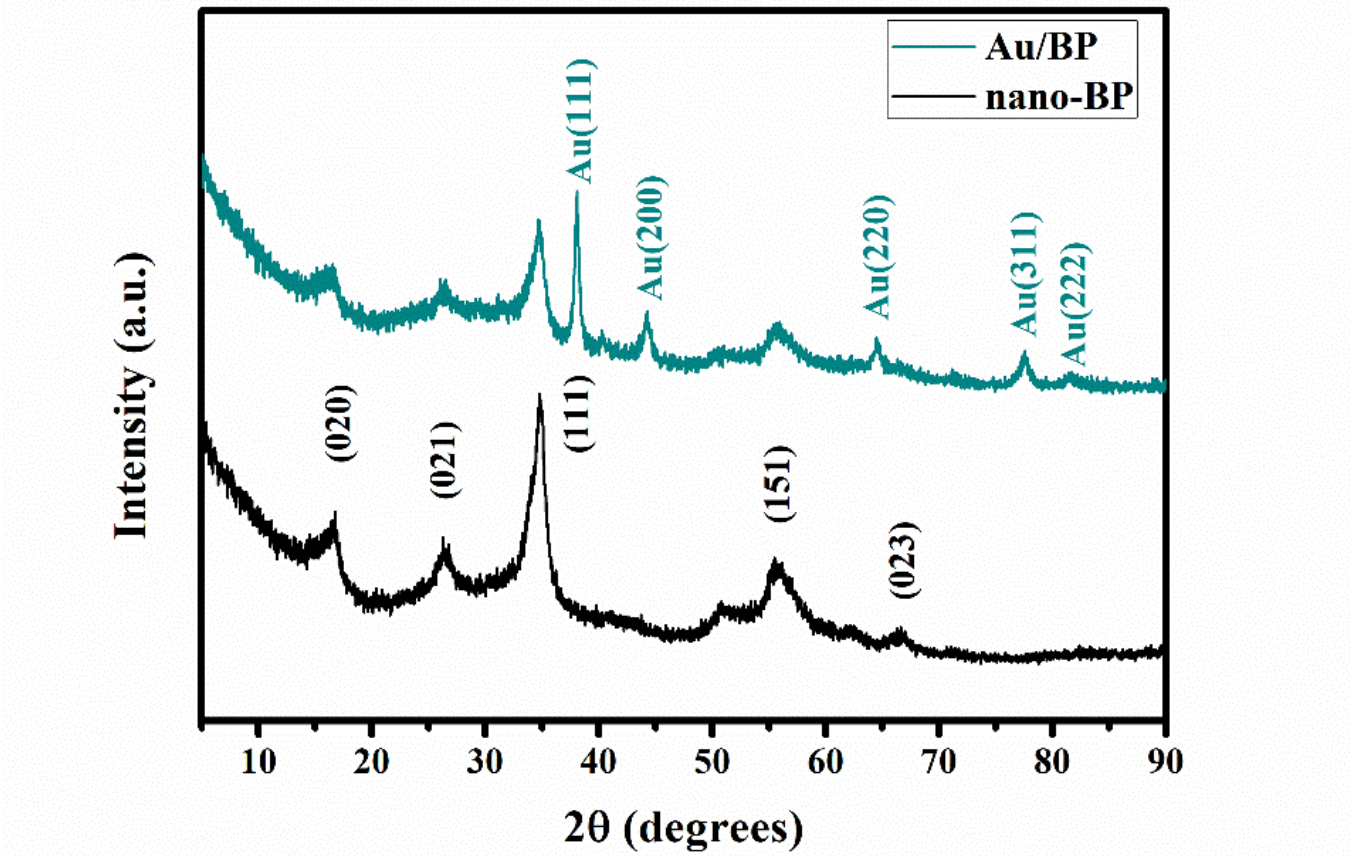

Figure 2S. XRD patterns of nano-BP and Au/BP. Figure 2S presents the XRD patterns of nano-BP and Au/BP. The diffraction peaks at 26.5°, 35.0°, and 56.0° correspond to the (020), (021), and (111) planes of black phosphorus, respectively. Compared to nano-BP, Au/BP shows diffraction peaks at 38.1°, 44.3°, 64.4°, 77.3°, and 81.5° corresponding to the (111), (200), (220), (311) and (222) planes of Au, respectively. These results indicate that BP and Au nanoparticles have the orthorhombic and cubic structures, respectively.

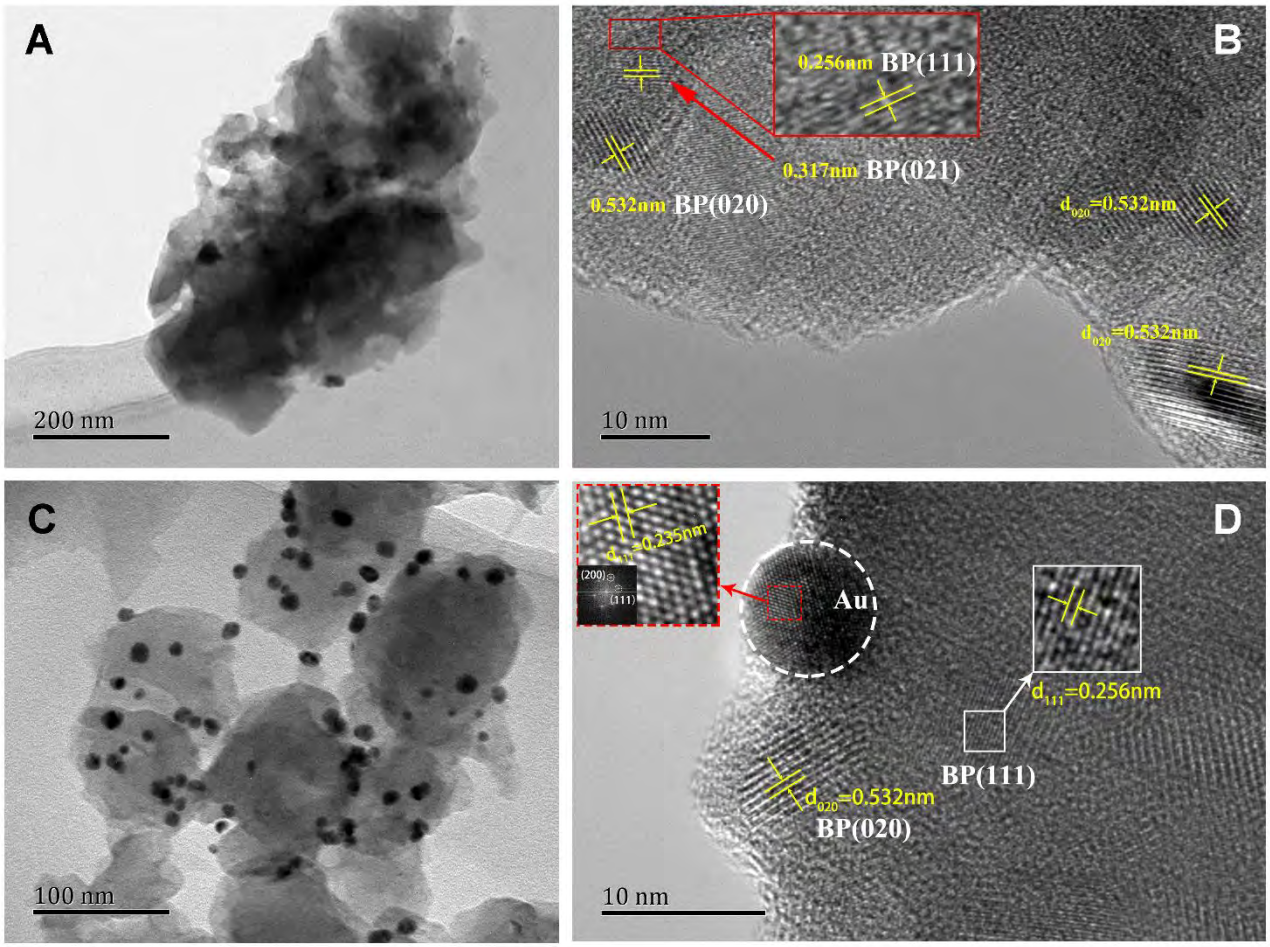

Figure S3. TEM images of (A, B) nano-BP, and (C, D) Au/BP (Inset in Figure 3B and d showing the locally enlarged view and the FFT pattern of Au in Figure S3D). Figure S3A shows that the size of nano-BP is approximately 200 nm. The crystal planes of (020), (021), and (111) for black phosphorus are shown in Figure S3B. The TEM images of Au/BP are depicted in Figure S3C, D. The size of nano-Au on the surface of BP is about 20 nm. The enlarged inset in Figure S3D shows the lattice spacings of Au and BP furnishing evidence that nano-Au is dotted on the BP surface.

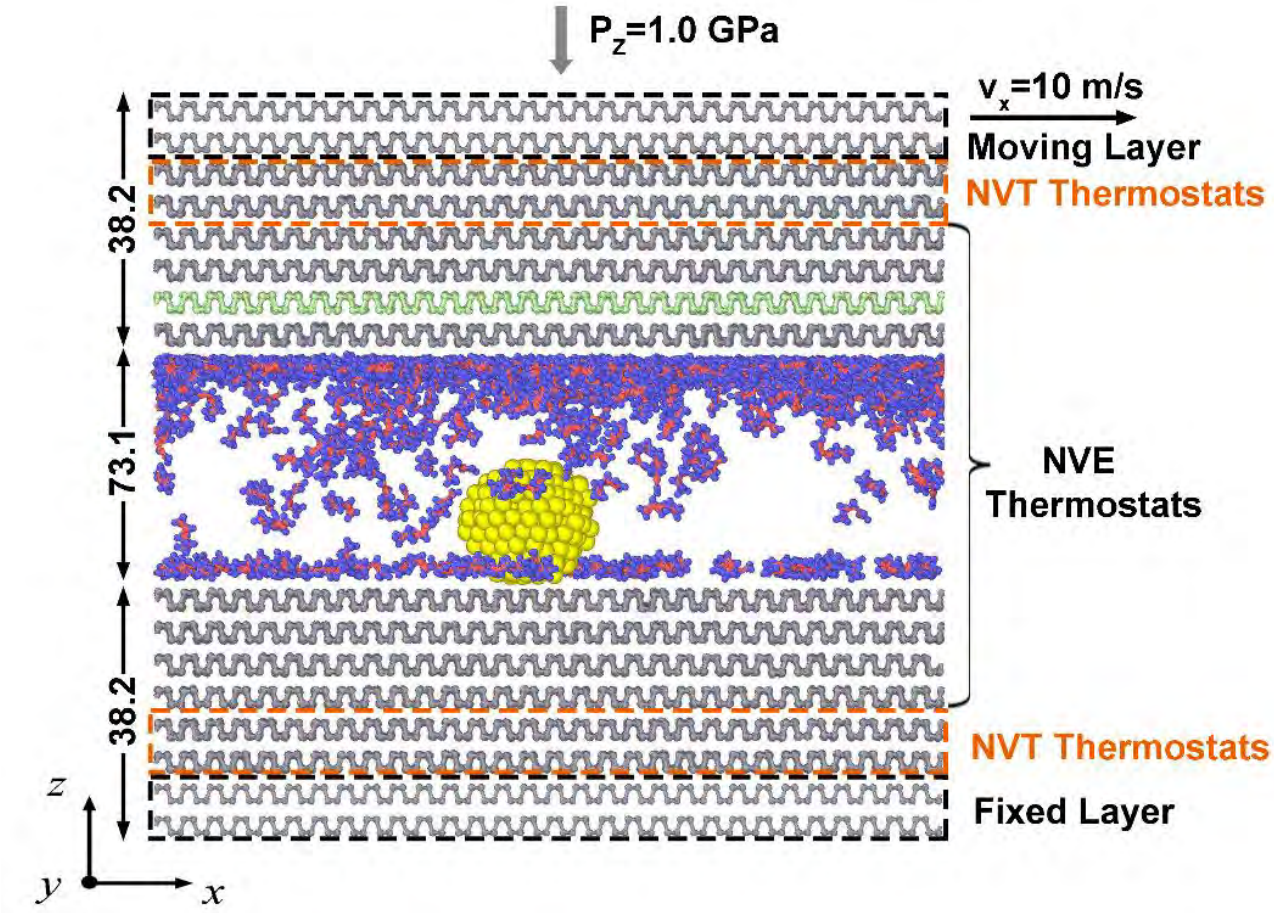

Figure S4. Schematic of the model used in MD simulation. The red, blue, gray and yellow atoms represent C, H, P and Au, respectively, and the friction force and stress distribution of the BP atoms in the cyan layer are calculated.